ARTICLE NO. 79-0598R

J80-146

00023
0001
0005

Bandwidth Attenuation with a Folded Cavity Liner in a Circular Flow Duct

D. T. Sawdy* and R. J. Beckemeyer†
Boeing Military Airplane Company, Wichita, Kansas

An extended reaction analysis is presented for investigating the bandwidth attenuation characteristics of a folded cavity resonator lining in a circular flow duct. An eigenfunction expansion technique was used to provide a multimodal extended reaction representation of the acoustic fields in the duct and resonator cavities. Using this method, computational studies were conducted to determine sensitivity of liner attenuation to changes of cavity geometry, and folded cavity configurations were identified that attenuate low frequency noise and that satisfy broadband attenuation requirements.

Nomenclature

$\bar{A}$ = specific wall admittance
a = height of internal baffle
a_n = expansion coefficient for incident modes
b = height of folded cavity
b_n = expansion coefficient for reflected modes
c = speed of sound
F_m = eigenfunctions for annular duct segment, order m
f = frequency, Hz
f_c = crossover frequency of linear impedance model
h = dimensionless duct height
i = $\sqrt{-1}$
J_m = Bessel function of first kind, order m
k = wave number
ℓ = length of face sheet
L = length of folded cavity
$\bar{L}$ = length of duct or cavity segment
M = Mach number of mean flow
p = dimensionless perturbation pressure
Q_m = weighting function for annular duct eigenfunction
R = face sheet impedance
r = dimensionless radial coordinate
S = interface surface
v = transverse component of dimensionless particle velocity
w = axial component of dimensionless particle velocity
Y_m = Neumann function, order m
y = dimensionless transverse coordinate
Z = specific impedance
z = dimensionless axial coordinate
ζ = dimensionless axial coordinate
λ = dimensionless modal propagation constant
μ = dimensionless modal eigenvalue
π_t = transmission loss, dB
ρ = mean density
$\phi, \bar{\phi}$ = acoustic field weighting functions
ψ = modal weighting function
ω = frequency, rad/s

Presented as Paper 79-0598 at the AIAA 5th Aeroacoustics Conference, Seattle, Wash., March 12-14, 1979; submitted April 16, 1979; revision received Dec. 26, 1979.

Index categories: Noise; Aeroacoustics; Computational Methods.

*Specialist Engineer, Noise Technology Staff.
†Research and Development Manager, Technology Staff.

I. Introduction

THE extended reaction model presented here for a folded cavity liner in a circular flow duct is the result of several years of research activity that has been directed toward development of analyses of lining concepts for broadband and/or low frequency noise reduction. The folded-cavity configuration is one in which the liner cavity is folded to lie parallel to the duct axis to provide a large reactive volume without the excessive liner depths required by conventional resonator liners. This nonconventional cavity arrangement has provided broad bandwidth attenuation performance for low frequencies in preliminary analyses and in model test programs that were conducted to evaluate several liner concepts. A simple locally-reacting (point-reacting[1]) impedance math model of the folded cavity liner that had been used to size the cavities failed to predict the measured attenuation performance. Consequently, a research activity was undertaken to understand the attenuation mechanisms of the folded cavity resonator and to develop analytical techniques to predict its sound power attenuation.

Several somewhat more sophisticated locally-reacting impedance models were developed[2] for the reactance of a two-dimensional folded cavity. Comparison of results of these models with experimental data showed them to be accurate only for a range of frequencies below that of design interest. Consequently, it was necessary to develop an extended-reaction theory. While the behavior of extended-reaction acoustic cavities in ducts has been successfully modeled by finite element[3] and finite difference[4] techniques, the present research activity involved the development of a multimode analysis based on familiar eigenfunction expansion techniques.[5-11]

Successful experimental verification of the two-dimensional model[2-11] prompted the extension of the eigenfunction expansion and boundary condition matching[10] techniques that had been developed for two-dimensional geometry to the case of circular geometry. As shown in Fig. 1, the folded cavity model consists of two annular resonating chambers that are separated from the lining chamber by a partial baffle. Lining chamber eigenvalues are calculated by a numerical algorithm developed for the case of a circular duct bifurcated by an acoustically porous face sheet with a uniform flow on one side and no mean flow on the other. These cavity elements were incorporated into a circular flow duct computer code[7] to form a multisegment extended-reaction duct analysis. In this paper, the extended-reaction model is described and results from computational studies of the model are presented. Results are also shown for computational predictions that were performed to identify folded cavity configurations that meet broadband attenuation objectives.

II. Theoretical Development

The problem of developing an extended-reaction analysis for a flow duct with a folded cavity resonator liner is resolved into a multiregion coupled boundary value problem. The geometry of this problem (Fig. 1) consists of a uniform cross-section, circular duct containing mean flow with the resonator lining and the acoustic excitation axisymmetric about the duct centerline. The model of the folded cavity liner consists of two annular resonating chambers that are separated from the lining chamber by a partial baffle.

The geometry of the present problem makes it amenable to efficient solution by the mode matching or eigenfunction expansion method. Since the boundaries of the duct and the resonator cavity correspond to coordinate surfaces of a cylindrical coordinate system for each region, the acoustic fields may be expressed in terms of cylindrical eigenfunctions which explicitly satisfy the Helmholtz equation and the wall boundary conditions.

The modal expansion for the pressure field in either a conventional duct segment resonating chamber, or a cavity lining segment is given in terms of right and left moving waves,

$$P=\sum_{n=0} a_n \vec{\psi}_n F_m(\vec{\mu}_n r) e^{-i\vec{\lambda}_n z} + \sum_{n=0} b_n \bar{\psi}_n F_m(\bar{\mu}_n r) e^{-i\bar{\lambda}_n \zeta} \quad (1)$$

where a_n and b_n are expansion coefficients for the incident and reflected modes, respectively. The axial coordinate z is referenced to the left-hand boundary of the section while $\zeta = z - \bar{L}$ is referenced to the right-hand side of the section and $\bar{L}$ is the section length. Steady state harmonic motion with a time dependence $e^{i\omega t}$ has been assumed. Linear coordinates are nondimensionalized by reduced frequency $k=\omega/c$ where ω is the excitation frequency in rad/s and c the speed of sound. Perturbation pressure is normalized by ρc^2 (ρ is the mean density) and particle velocity by the sound velocity.

Cylindrical eigenfunctions for the duct segments are Bessel functions $J_m(\mu_n r)$ of order m. The corresponding eigenvalues μ_n are determined from the boundary condition for a locally-reacting acoustically lined wall,

$$\frac{\partial p}{\partial r} - i\bar{A}(1-\lambda_n M)^2 p = 0 \quad (2)$$

which is derived by imposing continuity of acoustic particle displacement normal to the wall[9] ($\bar{A}$ is the specific acoustic admittance of the wall and M is the mean flow Mach number).

The axial dependence for the cavity and duct acoustic fields is specified in terms of the modal propagation constants λ_n which are related to the modal eigenvalues μ_n by

$$\mu_n^2 = [(1-\lambda_n M)^2 - \lambda_n^2] \quad (3)$$

Lining chamber segment eigenvalues (for both the duct and lining chamber portions of the segment) are calculated using a numerical algorithm developed for a duct bifurcated by an acoustically-porous face sheet with a uniform flow on one side and no mean flow on the other (Fig. 2). The transcendental equation for the bifurcated duct is

$$F_m^I(r_b)\frac{\partial}{\partial r}F_m^{II}(r_b)(1-\lambda M)^2 - F_m^{II}(r_b)\frac{\partial}{\partial r}F_m^I(r_b) - \frac{iR}{\rho c}\frac{\partial}{\partial r}F_m^{II}(r_b)\frac{\partial}{\partial r}F_m(r_b) = 0 \quad (4)$$

where

$$F_m^i(r) = J_m(\mu^i r) + Q_m^i Y_m(\mu^i r), \quad i = I, II$$

R is face sheet impedance, r_b is duct radius of face sheet, and

$$\mu^I = \mu^{II}\{[(1-\lambda M)^2 - \lambda^2]/[1-\lambda^2]\}^{1/2}$$

The Q_m^i are weighting functions defined as $Q_m^I = 0$ for region I (the duct) and

$$Q_m^{II} = \left[\frac{\partial}{\partial r}J_m[\mu^{II}(r_b+b)]\right] \Big/ \left[\frac{\partial}{\partial r}Y_m[\mu^{II}(r_b+b)]\right]$$

for region II (the lining chamber).

Equation (4) was derived by relating the acoustic fields on each side of the porous face sheet by use of the impedance characteristics of the sheet:

$$P^I - P^{II} = \frac{Rv^I}{\rho c} = \frac{Rv^{II}}{\rho c} \quad (5)$$

Weighting functions ψ_n for Eq. (1) are unity for the duct segments. For the cavity portion of the lining segment, the ψ_n, required to satisfy pressure and particle velocity boundary conditions at the acoustically porous face sheet, are given by:

$$\psi = F_m^I(r_b)/[F_m^{II}(r_b) + i\frac{R}{\rho c}\frac{\partial}{\partial r}F_m^{II}(r_b)] \quad (6)$$

Axial and transverse components of particle velocity are related to the acoustic pressure through the respective momentum relations

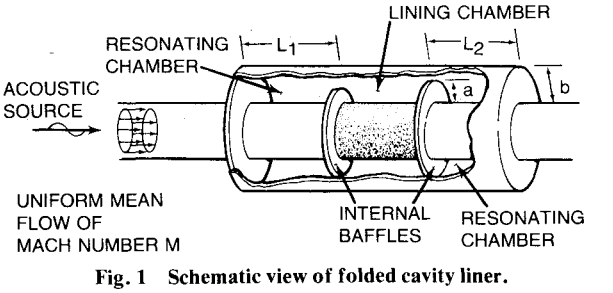

Fig. 1 Schematic view of folded cavity liner.

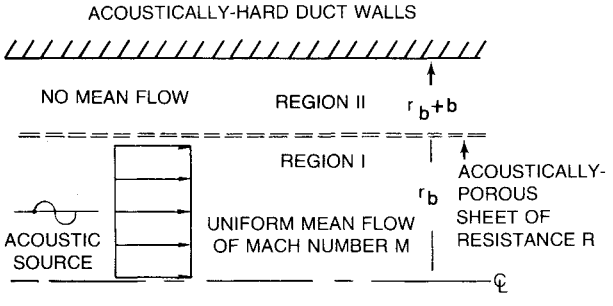

Fig. 2 Bifurcated duct model.

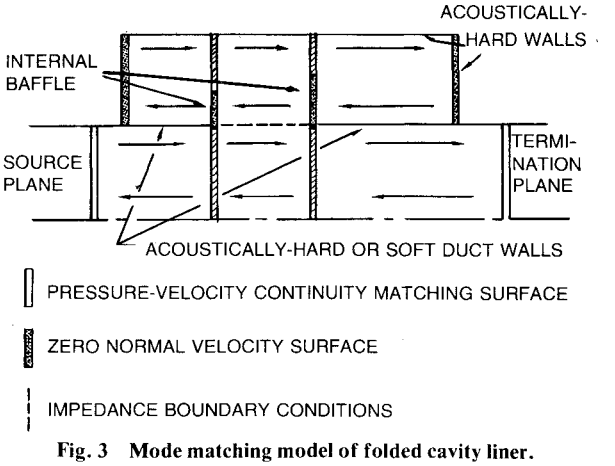

Fig. 3 Mode matching model of folded cavity liner.

$$u=\lambda p/(1-\lambda M) \tag{7}$$

$$v=i\frac{\partial p}{\partial r}\Big/(1-\lambda M) \tag{8}$$

Acoustic fields for the duct and cavity liner segments are coupled by using the mode matching method[10] to impose the requirements that the overall acoustic field be continuous (i.e., that successive segments have matching data at their interface) and that the kinematic conditions be satisfied on the transverse walls. Errors in pressure p^j-p^{j+1} and velocity u^j-u^{j+1} at the duct cross section between segments j and $j+1$ are minimized by the use of the method of weighted residuals. Pressure and particle velocity residuals are multiplied by appropriate weighting functions ϕ, $\bar{\phi}$ and integrated over the corresponding interface surface S

$$\int_S (p^j-p^{j+1})\phi ds=0 \tag{9}$$

$$\int_S (u^j-u^{j+1})\bar{\phi} ds=0 \tag{10}$$

to yield interface matching equations.

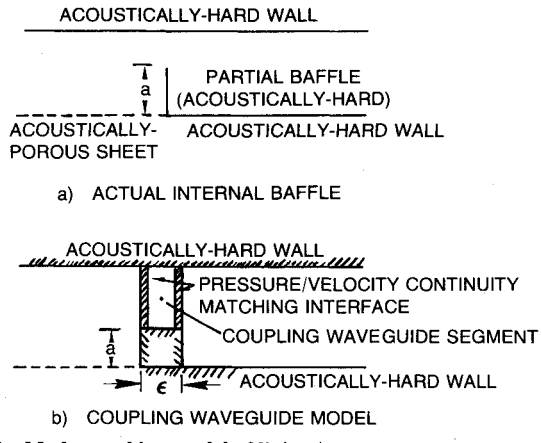

Fig. 4 Mode matching model of lining/resonator chamber interface.

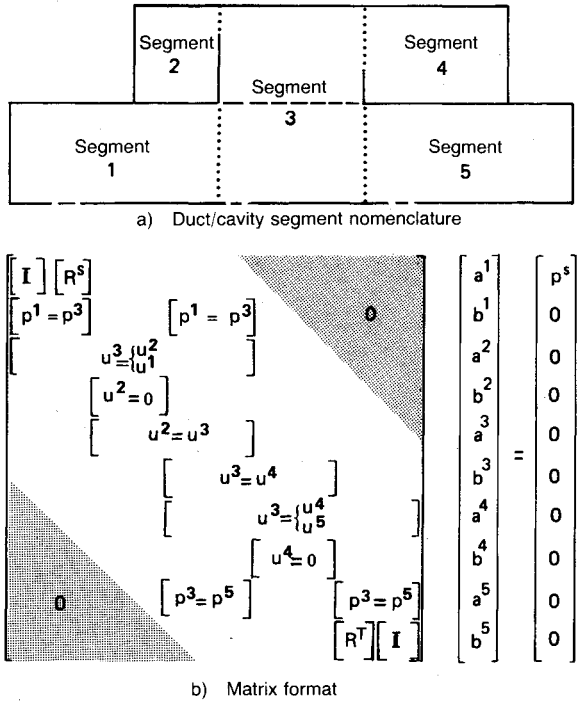

Fig. 5 Duct/cavity matching equations.

Interface equations for joining two uniform geometry, circular duct segments with different wall admittances have been documented by Zorumski[5] and consequently will not be presented here. For the present cavity analysis, the duct system consisted of five regions (Fig. 3). Mode matching equations for the cavity/duct interfaces required utilization of matching techniques for handling the particle velocity discontinuities on the interfaces containing transverse walls. These coupling equations required the derivation of original analytical techniques for matching the acoustic fields for wave guide segments separated by a partial baffle.

The problem of matching boundary conditions along the partial baffle and acoustic fields on its aperture resolves into adequately specifying a well-posed coupling boundary value problem. Two methods were developed to accomplish this matching numerically for the two-dimensional case. These techniques have been discussed in detail in a previous publication.[10] For the circular duct analysis, the coupling wave guide method[10] was used to model the interface containing the baffle (Fig. 4). Pressure and particle velocity continuity are imposed on both interfaces of the coupling waveguide segment. The axial components of the particle velocity fields in both the lining chamber and the resonating cavity are forced to vanish on the walls of the finite width baffle. It should be noted that the discontinuity in particle velocity at the top of the baffle can result in numerical problems in the determination of the acoustic field of the chambers and cavity.

Equations for the unknown modal expansion coefficients are obtained by truncating the field expansions, Eqs. (1) and (7), to a finite number of terms and using them in the interface matching Eqs. (9) and (10). These duct/cavity matching equations were combined with source and terminating equations to form a set of linear algebraic equations which are shown schematically in matrix form for a single folded cavity on Fig. 5. The solution vector is calculated by a banded matrix equations solver that utilizes a Gaussian elimination technique with partial pivoting.[12]

The modal expansion coefficients enable the truncated field expansions, Eqs. (1) and (7), to be used in the development of closed form expressions for energy flux and root mean square (rms) pressure in the duct segments. The energy flux expression presented by Morfey[13] was used to predict the acoustic energy transmission in the flow duct.

Math models for two types of face sheet materials, fiber-metal and conventional perforated plate, have been incorporated into the extended-reacting cavity models. The impedance of a fiber-metal face sheet was modeled by a simple crossover frequency expression.[9] Face sheet resistance was determined from the intercept and slope, (cgs RayL/cm/s), of dc flow resistance data. Based on un-

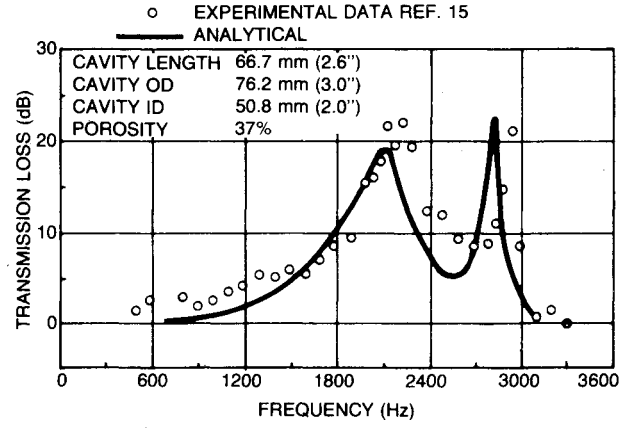

Fig. 6 Analytical-experimental correlation. Comparison of experimental and predicted transmission loss spectra for a concentric tube resonator.

published impedance tube test data for this type of material, a value of crossover frequency, $f_c = 15{,}000$ Hz was used in this study as a representative value for the fiber metal face sheet. Impedance characteristics for a perforated plate were modeled by use of nonlinear semiempirical expressions[14] that account for amplitude-dependent and grazing flow effects.

III. Results of Computational Studies

Computer codes were written to implement the analytical techniques developed during this research activity. They have been incorporated into a multilevel-overlay FORTRAN IV computer code that can analyze folded cavity liner configurations subject to the following restrictions: 1) flow profile is uniform in duct (no shear layer), 2) density and temperature of duct/cavity medium are uniform, 3) impedance surface of cavity element is uniform in circumferential direction, 4) only two folded cavity liners may be analyzed in series, 5) face sheet porosity must be the same for both cavity liners, and 6) baffles must be the same height for each cavity liner.

This computer code was used to evaluate the influence of cavity geometry changes on the bandwidth attenuation characteristics of the folded cavity liner. These computational studies were limited in scope to folded cavity configurations of fixed duct radius 15.2 cm (6 in.), fixed cavity height 10.2 cm (4 in.), no internal baffle $a = 0$ and to a flat input noise spectrum of 140 dB. In addition, source plane and termination plane reflections were ignored. Since the basic attenuation mechanism of the folded cavity liner is the reflection of acoustic energy rather than dissipation, acoustical interaction between the folded cavity liner and source and termination reflections would have to be accounted for in any attempt to provide a realistic model of an entire suppression system. Thus, it should be noted that results of the following computational studies are limited to defining the behavior of folded cavity configurations in the somewhat artificial environment of an infinite duct and, consequently, cannot be applied directly to estimate the

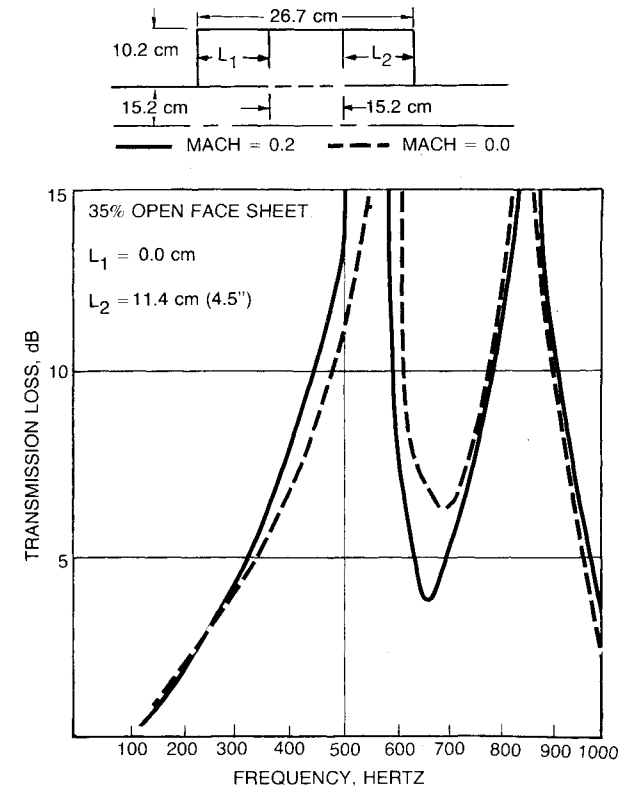

Fig. 7 Transmission loss spectra for a downstream cavity configuration with different Mach numbers.

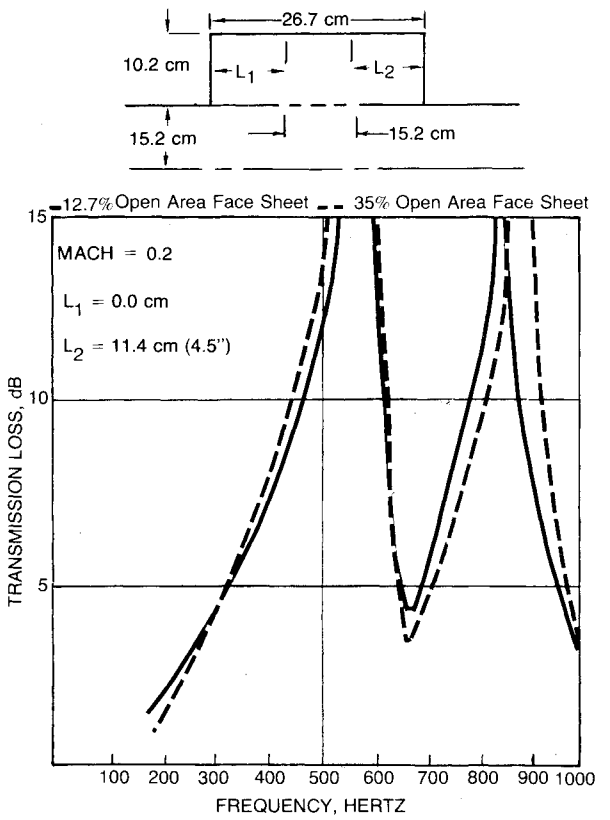

Fig. 8 Transmission loss spectra for a downstream cavity configuration with different face sheet open areas.

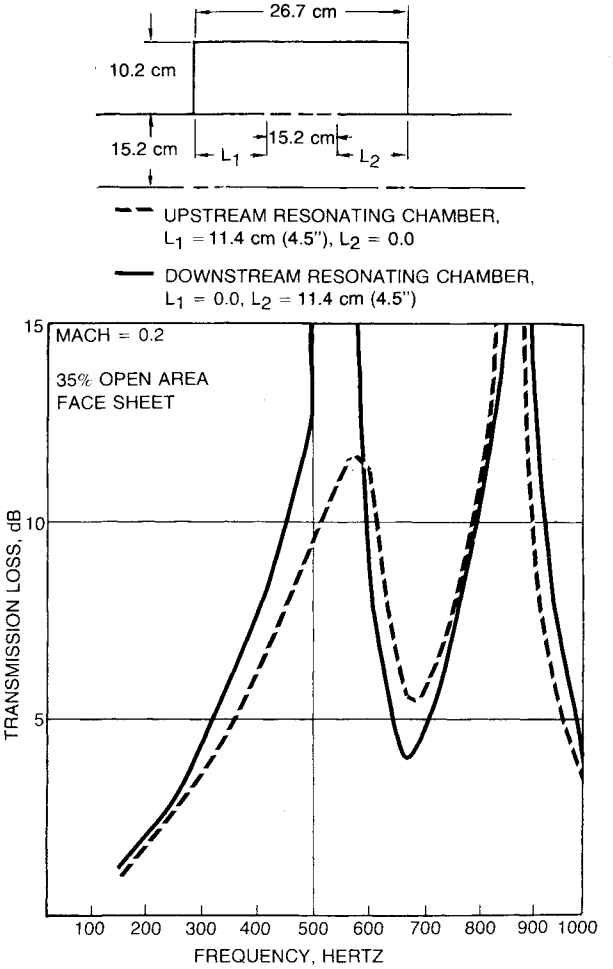

Fig. 9 Transmission loss spectra for folded cavity liners with an upstream resonating chamber configuration and a downstream resonating chamber.

performance of cavity configurations with source interactions or termination reflections.

Throughout the course of these analytical studies, the acoustic source was specified by the plane wave (zeroth angular, zeroth radial acoustic mode) in the left-hand (upstream) hard-walled segment. To ensure adequate representation of the acoustic fields, at least six terms were used in the eigenfunction expansions in each segment and eigenvalues for the lining chamber and duct segments were checked for completeness as well as for the presence of duplicate values.

The low frequency grazing flow duct facility[11] used to verify the two-dimensional analysis could not be used for the testing of a circular duct with an annular folded cavity liner. Therefore, experimental data were not available to validate the folded cavity model for circular geometry. However, experimental data[15] for a concentric tube resonator were available to provide verification of the analysis for a folded cavity configuration without a resonating chamber. The short resonator configuration (see Fig. 6 of Ref. 15) was analyzed with the folded cavity model for the case of zero mean flow and for the published values of face sheet parameters. The generally good agreement between theoretical and measured transmission loss spectra shown in Fig. 6 confirmed the capability of the extended-reaction model to predict the attenuation performance of a circular duct with an annular resonating cavity liner. To provide partial verification of the analysis for a folded cavity configuration, the accuracy of boundary matching was used as a measure of the validity of the analytical results. Pressure and particle velocity profiles were calculated on both sides of each interface to verify that the total acoustic fields were continuous, while particle velocity profiles were also calculated on each hard-walled boundary to verify the vanishing of particle velocity normal to that surface. Generally, quite good boundary matching was achieved.

Computational studies were made in an attempt to identify the influence of various geometric and physical parameters on folded cavity attenuation performance. The effects of Mach number on attenuation performance are shown on Fig. 7 (for 35% open area face sheet) to be negligible for the small values of Mach number studied. Figure 8 contains a comparison of transmission loss spectra for two different perforated face sheets (12.7 and 35% open area, and Mach = 0.2) and also shows that the actual resistance value for these low resistance face sheets does not significantly affect the attenuation spectrum for the cavity. These results are of interest because they verify trends seen in unpublished experimental test data. Since the folded cavity liner is primarily a reactive attenuator, this insensitivity to face sheet resistance would no longer be expected for cases with large resistance values.

Computational studies were also made to evaluate the influence of the relocation of the resonating chamber on the attenuation performance of the folded cavity liner. The comparison of transmission loss spectra for downstream and upstream resonating chamber configurations is shown on Fig. 9. (Mach = 0.2 and 35% open area face sheet). The location of the resonating chamber is shown to change the attenuation level of the low frequency attenuation peak. The lower attenuation associated with the upstream cavity appears to be related to the reduced communication between this cavity and the duct caused by the convection by the uniform duct flow.

The sensitivity of liner attenuation to each of the geometric parameters, cavity length, face sheet length, and arrangement of the resonating chambers was investigated separately. In

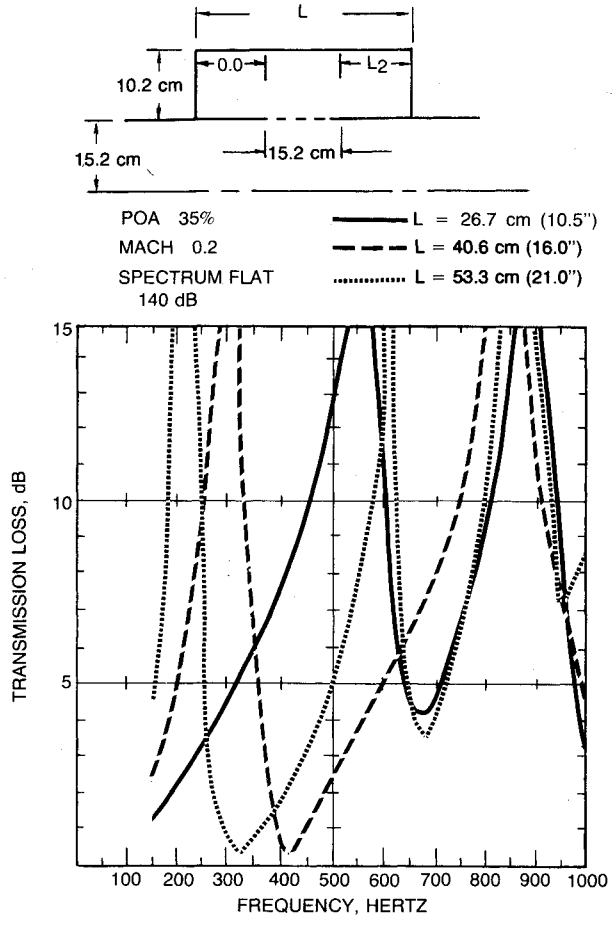

Fig. 10 Transmission loss spectra for single resonating chamber configurations with different total lengths.

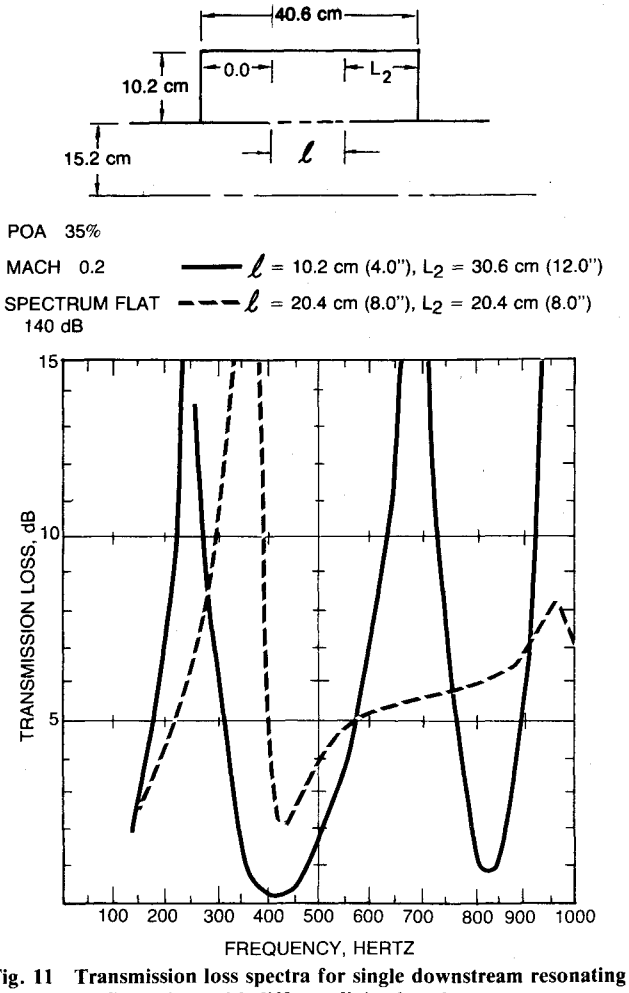

Fig. 11 Transmission loss spectra for single downstream resonating chamber configurations with different lining lengths.

varying total cavity length, cavity height and face sheet length were held constant. Transmission loss spectra for three different cavity lengths are shown on Fig. 10. All three configurations involve downstream cavities only. The frequency of the first attenuation peak for each case shifts in a predictable manner as the cavity length is changed. The lowest attenuation peaks occur at the resonant quarter wavelength frequencies based on cavity lengths while the higher 800 Hz peak corresponds in each case to the quarter wavelength frequency for cavity height.

Total cavity length and height are not the only geometric variables available for tuning the attenuation peak. Attenuation spectra for the configuration with the cavity length of 40.6 cm (16 in.) with different face sheet length, $\ell = 10.2$ and 20.4 cm (4 and 8 in.), respectively, are shown on Fig. 11. These spectra show that the proportion of total cavity length used for the resonator chamber significantly alters the reactive characteristics of the folded cavity liner. Because of the change in propagation characteristics of an acoustic wave in a lined segment as opposed to a hard-walled segment, the increase in face sheet length causes an effective decrease in wavelength in the cavity, thus causing an increase in tuning frequency of the attenuation peaks caused by cavity length. Furthermore, the increase in resistance and change of reactance caused by the increase in face sheet length causes decreases in peak attenuations as well as smoothing of the attenuation spectrum.

Another trend study was performed to evaluate the influence of the interaction between resonating chambers separated by a lining chamber on the attenuation performance of the folded cavity liner. Sound power attenuation spectra are presented on Fig. 12 for three lining configurations with the same total cavity length $L = 26.7$ cm (10.5 in.) for Mach = 0.2 and 35% open area face sheet. A comparison of the transmission loss spectra shows that the attenuation peaks are lower when a portion of the chamber is moved upstream, just as was true when the entire chamber was upstream. Note that the data in Fig. 12 indicate that the bandwidth characteristics of the double resonating chamber configuration might be adjusted to meet narrow and/or broadband attenuation objectives by appropriate positioning of the cavity with respect to the fact sheet. Figure 13 contains similar data for configurations with a total cavity length of 16 in.

The broadest attenuation bandwidth evident in the data shown thus far is approximately 5 dB for 1½ octave bands. Since the folded cavity elements exhibit highly tuned resonant behavior, it was of interest to attempt to arrange two single element liners in series in a configuration such that total attenuation performance would be enhanced. A candidate configuration was based on the attenuation spectra of two single cavities of Figs. 10 and 13. The overlap in the attenuation spectra of the configurations of 26.7- and 40.6-cm (10.5- and 16-in.) lengths indicates that it might be possible to combine these two liners to yield improved attenuation for the entire 250-1000 Hz range of frequencies. Figure 14 illustrates the excellent results obtained by placing the two cavities in series directly adjacent to one another. The attenuation

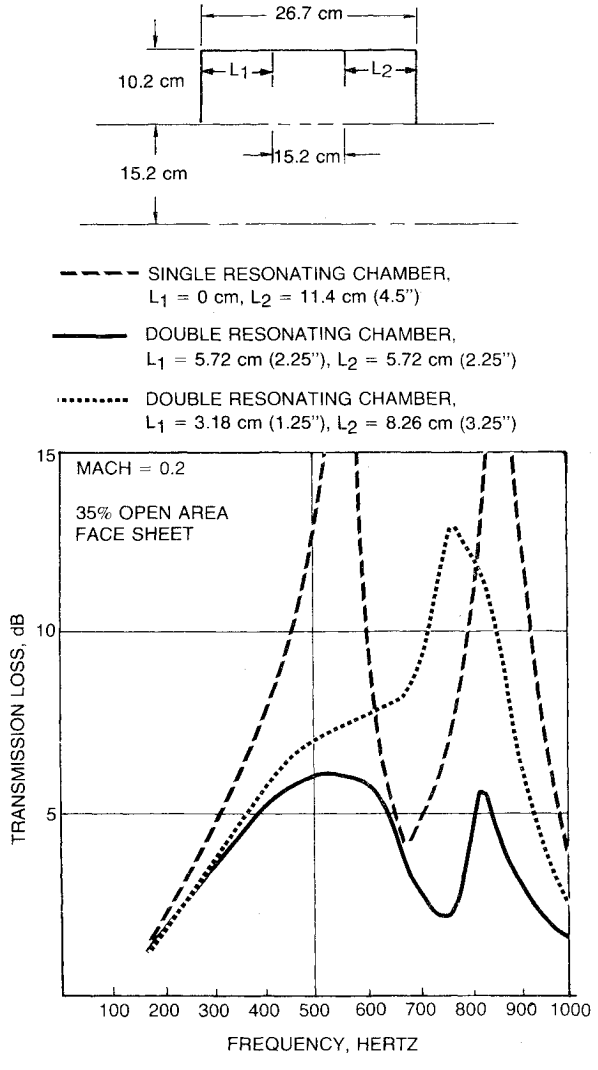

Fig. 12 Transmission loss spectra for a single resonating chamber and for two double resonating chamber configurations. Total cavity length held constant at 26.7 cm.

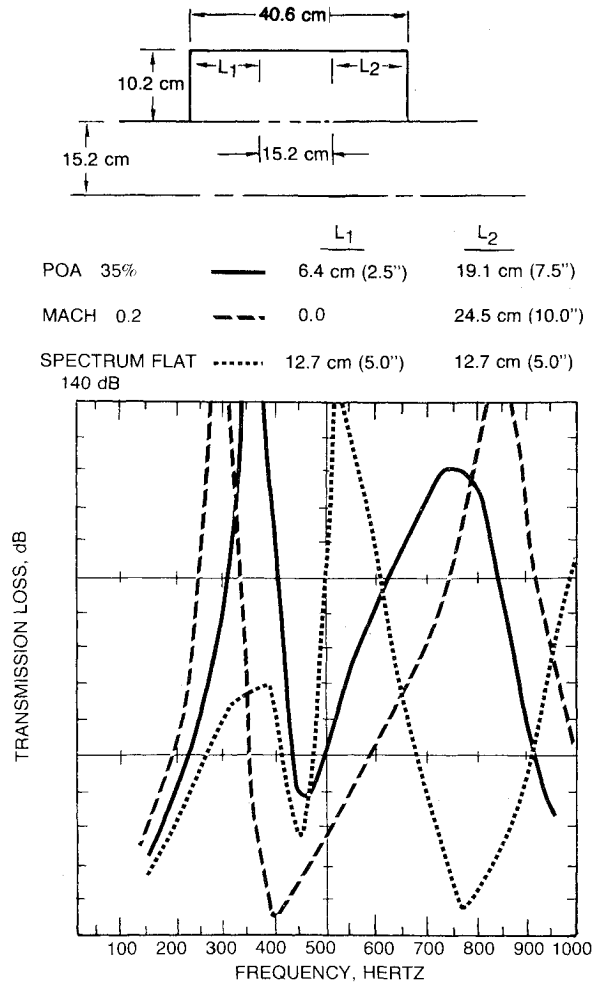

Fig. 13 Transmission loss spectrum for two double resonating chamber configurations and a single resonating chamber. Total length held constant at 40.6 cm (16.0 in.).

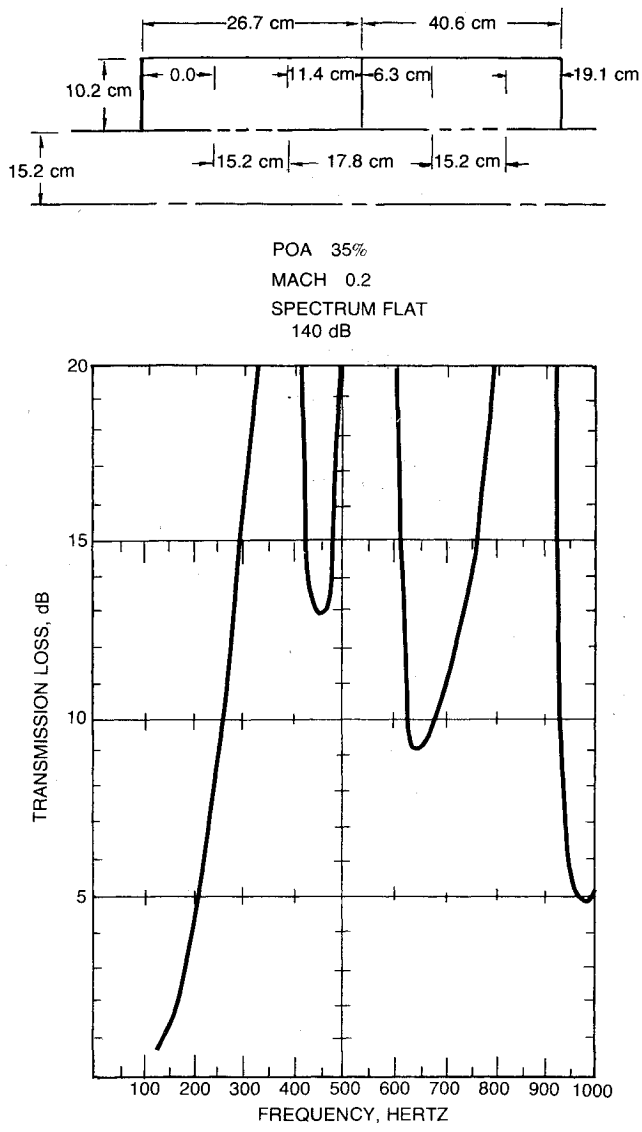

Fig. 14 Transmission loss spectrum for two folded cavity liners in series; liners contiguous.

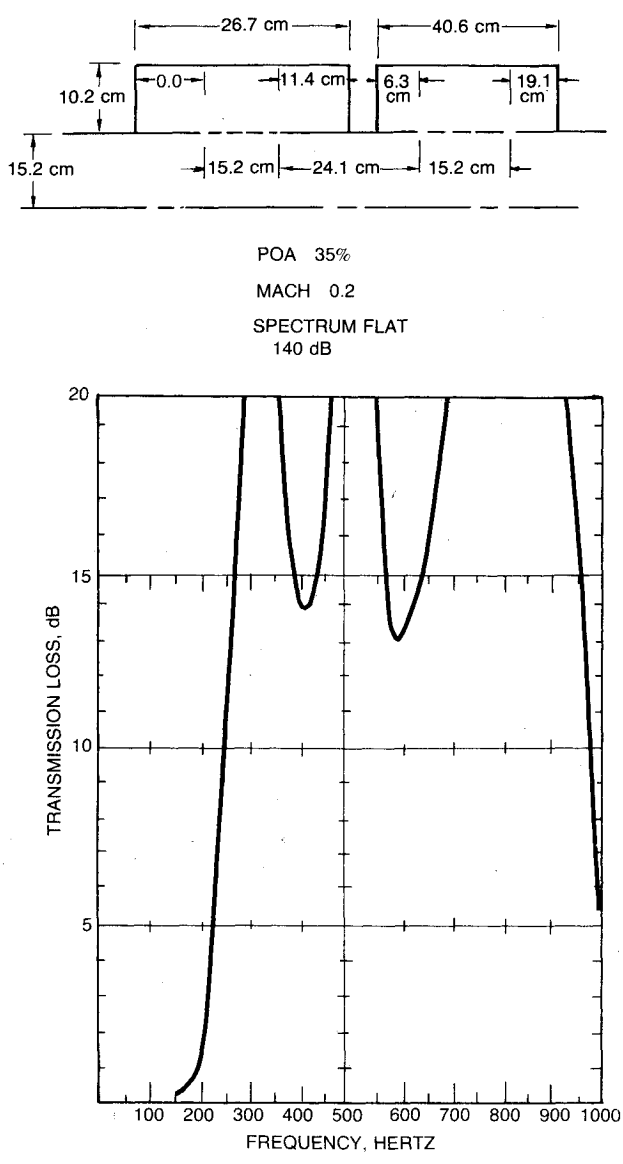

Fig. 15 Transmission loss spectrum for two folded cavity liners in series; liners set apart.

spectrum for this configuration is quite good, with at least 7 dB over two octave bands (200-1000 Hz). Results of a comprehensive trade study have shown that even more attenuation can be obtained by spacing the two cavities a certain distance apart. Figure 15 gives an attenuation spectrum for a configuration with two single cavity liners spaced 6.4 cm (2.5 in.) apart. This gap enhanced interaction between the cavities and provided an attenuation spectrum of 13-14 dB over two octaves (250-1000 Hz). The excellent performance of this configuration illustrates the capability of the extended reaction analysis to find optimum resonator configurations that can lead to improved design.

The two-element folded cavity configuration on Fig. 15 is the result of many iterations of a trial and error analysis procedure. With the large-scale computer technology currently available, it would seem desirable to develop a highly automated design procedure for the selection of a two-element configuration that provides maximum attenuation over a specified frequency bandwidth. Experience gained in this investigation, however, has shown that a highly automated design procedure requires a large and complex computer program. It appears that a trial and error procedure where the designer plays an active role in editing the liner attenuation performance is the most practical manner to select a folded cavity configuration that meets the attenuation objectives.

IV. Conclusions

Numerical results presented in this paper indicate that with a judicious choice of geometry, folded cavity resonator liners can be designed to provide broadband, low frequency attenuation. While a single element folded cavity liner with its highly tuned resonant behavior may not produce a sufficiently broad attenuation spectrum, two of these elements arranged in series can definitely be used to obtain substantial attenuation over a broad frequency band. Results of these computational studies are limited to defining the behavior of folded cavity configurations in the artificial environment of an infinite duct and, consequently, cannot be applied directly to estimate the performance of cavity configurations with source interactions or termination reflections.

Acknowledgments

This research is part of an independent research and development effort of the Boeing Military Airplane Company.

References

[1] Nayfeh, A. H., Kaiser, J. E., and Telionis, D. P., "Acoustics of Aircraft Engine-Duct Systems," *AIAA Journal*, Vol. 13, Feb. 1975, pp. 130-153.

[2] Beckemeyer, R. J. and Sawdy, D. T., "Analytical and Experimental Studies of Folded Cavity Duct Acoustic Liners," Paper YY11, Acoustical Society of America, San Diego, Calif., Nov. 1976.

[3] Craggs, A., "A Finite Element Method for Damped Acoustic Systems: An Application to Evaluate the Performance of Reactive Mufflers," *Journal of Sound and Vibration*, Vol. 48, Oct. 1976, pp. 377-392.

[4] Kurze, U., "Sound Propagation in a Duct of Periodic Wall Structure," Translation for *Acustica*, Vol. 21, 1969, pp. 74-85.

[5] Zorumski, W. E., "Acoustic Theory of Axisymmetric Multisectioned Ducts," NASA TR-R-419, 1974.

[6] Beckemeyer, R. J., Sawdy, D. T., and Garner, P., "Computational Methods for Acoustic Radiation from Circular Duct," *Aeroacoustics: Fan Noise and Control; Duct Acoustics: Rotor Noise*, edited by I. R. Schwartz, MIT Press, Cambridge, Mass., 1976, pp. 433-450.

[7] Sawdy, D. T., Beckemeyer, R. J., and Garner, P., "Effects of a Conical Segment on Sound Radiation from a Circular Duct," *Aeroacoustics: Fan Noise and Control; Duct Acoustics: Rotor Noise*, Edited I. R. Schwartz, MIT Press, Cambridge, Mass., 1976, pp. 433-450.

[8] Beckemeyer, R. J. and Sawdy, D. T., "Optimization of Duct Acoustic Liners of Finite Length," *Journal of the Acoustical Society of America*, Vol. 57, Suppl. No. 1, S16(A), Spring 1975.

[9] Sawdy, D. T., Beckemeyer, R. J., and Patterson, J. D., "Analytical and Experimental Studies of an Optimum Multisegment Phased Liner Noise Suppression Concept," NASA CR-134960, May 1976.

[10] Beckemeyer, R. J. and Sawdy, D. T., "Boundary Conditions for Mode-Matching Analyses of Coupled Acoustic Fields in Ducts," *AIAA Journal*, Vol. 16, Sept. 1978, pp. 912-918.

[11] Sawdy, D. T. and Beckemeyer, R. J., "Transmission Loss of a Folded Cavity Liner as Predicted by an Extended Reaction Analysis," AIAA Paper 77-1358, Atlanta, Ga., Oct. 1977.

[12] *System 360 Scientific Subroutine Package (360A-CM-03X) Version III*, Programmers Manual, 1966-68 IBM Corp., White Plains, N.Y.

[13] Morfey, C. L., "Acoustic Energy Flux in Nonuniform Flows," *Journal of Sound and Vibration*, Vol. 14, Dec. 1971, pp. 159-170.

[14] Armstrong, D. L., "Acoustic Grazing Flow Impedance Using Waveguide Principles," NASA CR-120848, 1971.

[15] Sullivan, J. W. and Crocker, M. J., "Analysis of Concentric-tube Resonators Having Unpartitioned Cavities," *Journal of Acoustical Society of America*, Vol. 64, July 1978, pp. 207-215.